Fibers and Polymers 2009, Vol.10, No.4, 513-518 DOI 10.1007/s12221-009-0513-y

Thermal and Mechanical Properties of Polypropylene Filaments Reinforced with Multiwalled Carbon Nanotubes via Melt Compounding

Soohee Choi, Youngjin Jeong*, Geon-Woong Lee[1], and Dae Hwan Cho[2]

Department of Oranic Materials and Fiber Engineering, Soongsil University, Seoul 156-743, Korea
[1]Korea Electrotechnology Research Institute, Changwon 641-120, Korea
[2]School of Chemical and Biomolecular Engineering, Cornell University, Ithaca, NY 14853, USA
(Received September 18, 2008; Revised April 27, 2009; Accepted May 1, 2009)

Abstract: This study examined the thermal and mechanical properties of polypropylene filaments reinforced with multi-walled carbon nanotubes (MWNTs). The MWNTs were functionalized with maleic anhydride polypropylene to increase the interfacial interactions between the CNTs and polypropylene. PP/MWNT composites with different concentrations of MWNTs were prepared by melt compounding using a twin screw extruder. The composites of the filament were then post drawn and heat treated. Tensile tests showed increased strength with the addition of only 0.1 wt% while there were only slight changes in elongation. The thermal properties were also slightly enhanced by the MWNTs.

Keywords: Carbon nanotube, Polypropylene, Melt mixing, Filament, Nanocomposite

Introduction

Carbon nanotubes (CNTs) are graphitic sheets rolled into seamless tubes (i.e., arrangements of carbon hexagons into tube-like fullerenes). CNTs have diameters ranging from approximately one nanometer to tens of nanometers and lengths in the micrometer range. Theoretical predictions have suggested carbon nanotubes to have remarkable mechanical properties with the Young's modulus of individual CNT in the order of TPa and a tensile strength as high as 200 GPa [1]. Due to these outstanding mechanical properties and high aspect ratio, CNTs have been considered to be ideal fillers in polymer composites [1-3]. However, most attempts at finding applications have identified several technical difficulties, such as poor dispersion and weak interfacial bonding, which are essential for realizing the full potential of nanotubes as reinforcing agents. One of the most efficient ways of increasing the dispersibility is the chemical functionalization of CNTs, which also enhances the interfacial bonding between the nanotube and polymer interface. The increased interfacial binding effectively transfers a load from a polymer matrix to the CNTs. Therefore, it is essential to functionalize the CNTs in order to exploit their merits in polymer composites.

Until now, most functionalization on CNTs has been achieved by introducing carboxylic acid groups (-COOH) using nitric acid oxidation [4-7]. However, it is very difficult to disperse CNTs grafted with carboxylic acid groups (-COOH) into a non-polar matrix, such as polypropylene (PP). The aim of this study was to disperse CNTs into PP, and increase the interfacial bonding between the CNTs and PP matrix. In addition, a fiber system was prepared with a CNT/PP composite, and the mechanical and thermal properties of the fiber system were examined at different CNT concentrations.

*Corresponding author: yjeong@ssu.ac.kr

Experimental

Materials

Multiwalled carbon nanotubes with ≥95 % purity, a diameter of 10-20 nm and a length of 10-50 μm were purchased from Iljin Nanotech Co., Korea. Maleic anhydride polypropylene (MA-g-PP) and polypropylene were supplied by Honam petrochemical Co., of Korea. The graft rate of maleic anhydride (MAH) was approximately 5 wt %, and the melt index (230 °C, 2.16 kg) of PP was 4.0 (model Y-130).

Pre-treatment of the MWNTs

Figure 1 shows a schematic diagram of the overall experimental procedure. The MWNTs were first oxidized to achieve improved compatibility with MA-g-PP. The MA-g-PP/MWNTs and neat MWNTs were mixed separately into a PP matrix using a high shear force. The following show the treatment conditions used in this study:

(i) Nitric acid treatment (MWNT-COOH): A 500 m*l* flask charged with 100 mg of neat MWNTs and 400 m*l* of 7M nitric acid was ultrasonicated for 2 hrs using a Sonics &

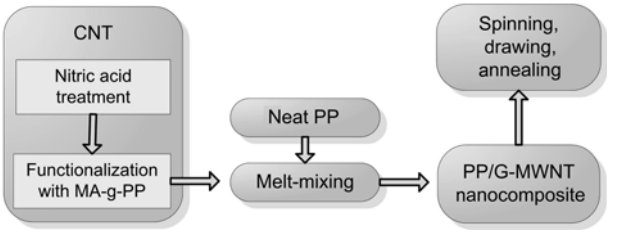

Figure 1. Schematic diagram of the experimental scheme used in this study.

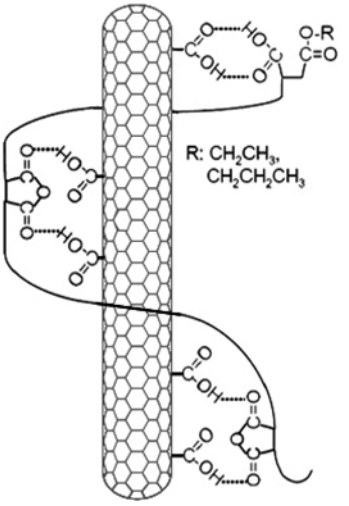

Figure 2. Schematic diagram of the interaction between the MWNT-COOH and MA-g-PP.

Materials Inc. bath sonicator (20 kHz, 150 W). The mixture was then stirred at 90 °C under reflux for 2 hrs. The solution was cooled to room temperature, and diluted several times with de-ionized water until the pH was approximately 7. Finally the solution was then filtered through a 8 μm pore cellulose filter paper, and dried for one week in a freeze drier.

(ii) Functionalization of the MWNTs with MA-g-PP: The acid treated MWNTs (MWNT-COOH) (0.05 g) were ultrasonicated in ethanol (500 m*l*) for 4 days. MA-g-PP (100 mg) was dissolved and stirred for 1 hr in Xylene (100 m*l*) under reflux. The MWNT suspension was dropped into the MA-g-PP solution and stirred for 90 minutes. During this process, the MWNT-COOH was expected to interact with the MA-g-PP, as shown in Figure 2. Finally, the solvent of the mixture was removed using a rotary evaporator to yield a gray powder of G-MWNTs.

Preparation of PP/G-MWNTs Nanocomposite Filaments

Nanocomposites were created by dry blending PP powder with a given ratio of G-MWNTs (0, 0.1, 0.5, 1.0 wt %). The pre-blends were mixed mechanically using basic analytical mill (IKA, A11) and fed into a twin screw extruder (Bautek, BA11, Korea) having a screw length to screw diameter (L/D) of 40. The temperature profile, starting from the feeding zone to the die, was 120 °C, 165 °C, 168 °C, 170 °C, 173 °C, 175 °C and its screw speed was 150 rpm. The extrudates of the PP/MWNT filaments were wound onto a winding apparatus at a rate of 30 rpm and postdrawn to a 6:1 draw ratio at 95 °C using a drawing machine designed by Ajin Machine Co., Korea. Subsequently, the drawn filaments were annealed at 120 °C for 2 hrs.

Measurements

FT-Raman spectroscopy (Bruker Equinox 55 FT-Raman Spectrometer) was used to characterize the chemical modification of the functionalized MWNTs using an Ar^+ incident laser with a wavelength of 514.5 nm and power of 36 μW. The infrared spectra were recorded on a Jasco FT/IR-6300 in KBr tablets. In addition, thermogravimetric analysis (Dupont Instruments TGA 2950 analyzer) was carried out by ramping the temperature from 30 °C to 600 °C at a heating rate of 10 °C/min under a nitrogen atmosphere. For the differential scanning calorimeter study (Perkin Elmer DSC-7), the samples were heated from 40 °C to 200 °C at heating rate of 10 °C/min under a nitrogen atmosphere, held at 200 °C for 5 min, then cooled to 80 °C at 10 °C/min.

A Hounsfield Universal Testing Machine (model H10k-S) was used to examine the mechanical properties of the PP/G-MWNT filaments using a load cell with a 50 kN capacity. The gauge length between the jaws at the start of each test was adjusted to 50 mm, and the measurements were carried out at a crosshead speed of 50 mm/min. The average of at least ten sample measurements was taken to represent each data point.

Field emission scanning electron microscopy (FE-SEM, JSM 6500F, Sirion 400, FEICOMPANY) operated at 15 kV was used to observe the microscopic dispersion of the MWNTs on a fractured surface of the nanocomposite filament as well as the morphology of the functionalized MWNTs.

Results and Discussion

Characterization of Pre-treated MWNTs

Using the acid treatment, the neat MWNTs were functionalized with carboxyl groups, which would contribute to the enhanced dispersion of CNTs in the water or organic medium. The oxidized MWNTs were ultrasonicated in ethanol before being reacted with MA-g-PP. Figure 3 shows that the solution containing the MWNT-COOH remained stable for more

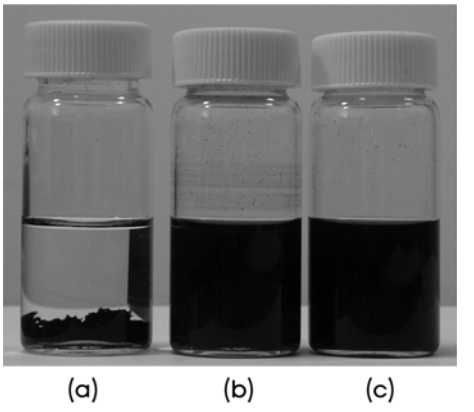

Figure 3. Dissolution experiments on the nanotubes in ethanol and ethanol/xylene. The neat MWNTs in ethanol (left) settled immediately after sonication. The acid functionalized MWNTs in ethanol (middle) and ethanol/xylene (right) did not show any visible changes for more than 48 hours.

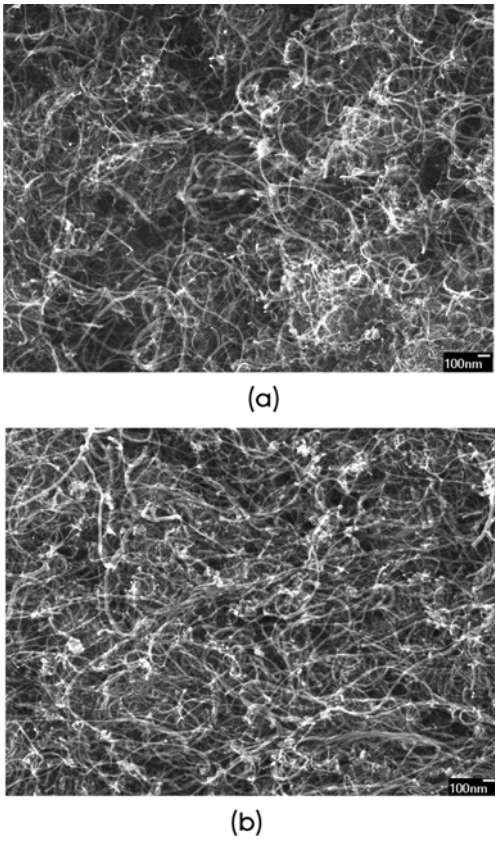

Figure 4. SEM images of (a) neat MWNTs and (b) acid treated MWNTs (×30,000).

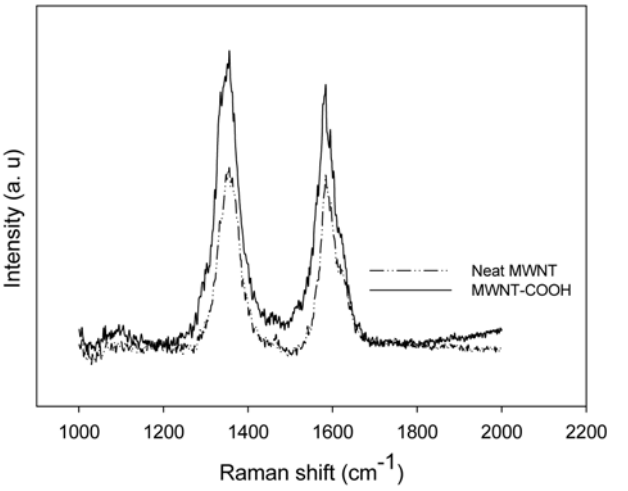

Figure 5. FT-Raman spectra of (a) neat MWNTs and (b) acid treated MWNTs obtained at 514.5 nm.

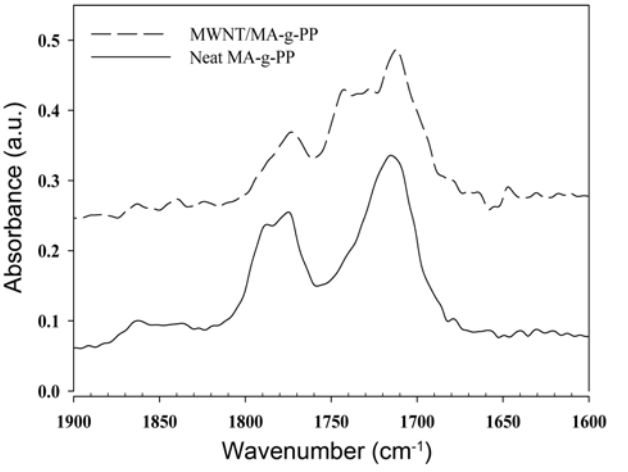

Figure 6. FTIR spectra of MWNT/MA-g-PP and neat MA-g-PP.

than 48 hours. However, the neat MWNTs ultrasonicated in ethanol settled immediately, as shown in Figure 3(a). In addition, the acid functionalized MWNTs remained well dispersed in the mixed ethanol and xylene solution (5:1), which was used as the solvent to react the MWNT-COOH with MA-g-PP.

The morphology of MWNT-COOH was compared with that of neat MWNTs to determine if the oxidized MWNTs had been damaged. The FE-SEM images in Figure 4 show that the two types of MWNTs were similar, which suggests that the treatment did not damage the oxidized MWNTs.

FT-Raman spectra in Figure 5 shows two major peaks in the high frequency range; the tangential mode or so-called G-band at 1580 cm^{-1} and the D-band at 1350 cm^{-1}, which was assigned to carbonaceous compounds or defects in CNTs. The ratio of the intensity of the D-band to G-band in MWNT-COOH is widely accepted as evidence of sidewall functionalization [8,9] because an increase in the number of sp^3-hybridized carbon atoms suggests that some species are bonded covalently to the nanotube framework. In this treatment condition, the ratio increased from 1.00 for the neat MWNTs to 1.17 for the acid treated MWNTs.

The neat MA-g-PP spectrum (Figure 6) shows strong absorbance for polymaleic anhydride (1784 cm^{-1}) and the carboxylic acid C=O stretch (1715 cm^{-1}) with self-hydrogen-bonded carboxyl groups (COOH) [10]. The absorbance of the polymaleic anhydride stretch (1784 cm^{-1} peak) was down shifted in the MWNT/MA-g-PP and its relative intensity was reduced. This was attributed to the formation of hydrogen bonds between the polymaleic anhydride and MWNT-COOH [11].

Dispersion of MWNTs in Polymer Composites

A homogeneous dispersion of MWNTs in the polymer matrix is one of the most important properties for preparing a composite with the required mechanical strength. In order to observe the dispersion of MWNTs in the matrix, cross-sections of the composites were prepared by fracturing the MWNT/polypropylene composites in liquid nitrogen to produce an intact fractured surface morphology. Figure 7 shows the resulting SEM images, where the left figure (a) shows a fractured surface of the composite reinforced with

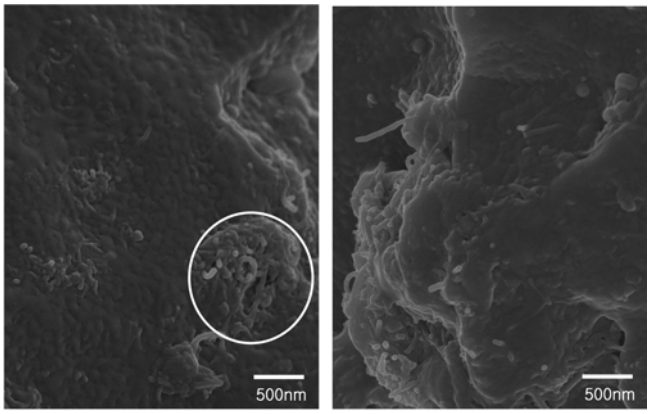

Figure 7. Cross section SEM images of the composites fractured at liquid nitrogen temperature for polypropylene composite containing 1.0 wt% (a) neat MWNTs and (b) functionalized MWNTs (×20,000). The circles in (a) show the nanotube aggregate.

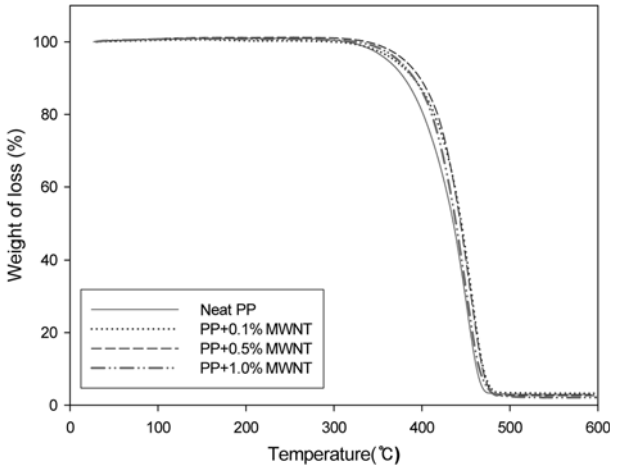

Figure 8. TGA curves of the PP/MWNT composites with different MWNT contents under a nitrogen atmosphere.

neat MWNTs (1.0 wt %). The nanotubes existed in the form of a highly entangled cluster. On the other hand, Figure 7(b) shows a well dispersed fractured surface of the composite reinforced with the functionalized MWNTs (1.0 wt %). This suggests that functionalization contributes to the dispersion of MWNTs in a polymer matrix.

Thermal Properties of the Composites

Figure 8 shows typical TGA curves of PP and PP/G-MWNT composites with different MWNTs contents under nitrogen atmosphere. The figure suggests that the MWNTs improve the thermal stability of PP under a nitrogen environment, even though the relationship between the amount of loaded MWNTs and the degradation temperature is unclear. The increased thermal stability appears to be due to the improved interaction between the MWNTs and PP and the improved dispersion by the MA-g-PP/MWNTs [12]. According to Marosfi *et al.* [12], improved interfacial interaction increases the activation energy of degradation at interface between the MWNTs and PP and retards the degradation at the surface of the composite owing to the superior thermal conductivity of the CNTs.

DSC measurements were performed to determine the thermal properties of the PP/MWNT composites. The results are shown in Table 1 and Figure 9. The results show that the

Table 1. DSC Data of the neat PP and PP/MWNT composites

Sample	Peak melting temperature (^oC) T_m	Crystalline temperature (^oC) T_c	Enthalpy (J g^{-1}) ΔH_m	Crystallinity (%)
Neat PP	163.37	115.03	88.34	42.65
0.1 %	163.10	117.80	92.01	44.43
0.5 %	163.87	119.00	92.44	44.64
1.0 %	162.83	119.57	92.75	44.78

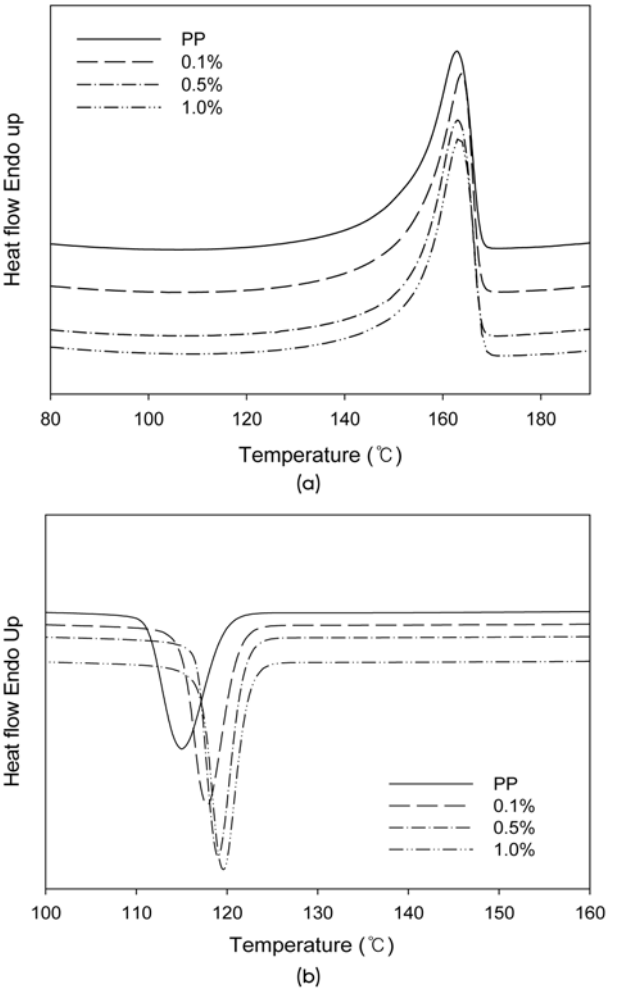

Figure 9. DSC graph of the PP/MWNTs composites with different MWNT concentrations; (a) heating results and (b) cooling results.

heat of fusion of the PP with MWNTs is slightly higher than that of the sample without the MWNTs. This suggests that more ordered polymer packing was obtained for the PP/MWNTs composites. This may be due to the presence of MWNTs, which enhances the crystallization process. The change in crystallinity due to the incorporation of MWNTs (Table 1) supports this explanation, where the crystallinity was calculated using a ΔH_f^0 value of 207.1 J/g for 100 % crystalline PP [13] and equation (1) (ΔH is the enthalpy measured from the experiment). Indeed, crystallization in a polymer involves primary nucleation and relatively rapid spherulitic growth [14]. Therefore, the crystallization temperature of PP/MWNTs is strongly affected by the incorporation of MWNTs. Some inorganic fillers, such as glass fiber, clay, carbon black, etc, incorporated into a polymer matrix act as nucleation agents to accelerate crystallization. Therefore, the crystallization behavior of a semi-crystalline polymer would be affected by the MWNTs. Table 1 shows that the crystalline temperature increased by approximately 4.5 °C with 1.0 wt% of the MWNTs compared with the neat PP.

$$\text{Crystallinity (\%)} = \frac{\Delta H}{\Delta H_f^0} \times 100 \quad (1)$$

Mechanical Properties of the Composites

Tensile tests for a single filament were carried out using a universal testing machine. Figure 10 shows the tensile strength and breaking elongation for the PP/MWNT filaments with different MWNT loadings. The results clearly show that the tensile strength is increased by the presence of MWNTs. However, the breaking elongation changed only slightly after adding the MWNTs. The tensile strength increased approximately 20 % at a 0.1 wt % MWNT loading, which supports both good dispersion of the MWNTs and effective load transfer from the polymer matrix to the MWNTs. However, the strength did not increase further at higher MWCNT concentrations. This is likely to be the result of a decrease in the dispersion of MWNTs in the polymer matrix with increasing MWNT concentration [15, 16]. These results are also in line with the increased crystallinity of the PP/MWNT composites.

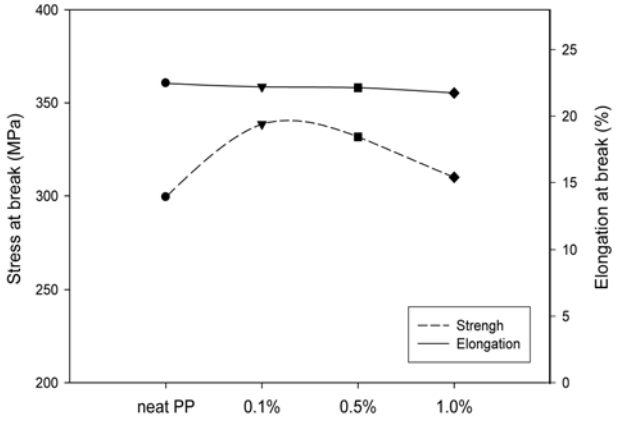

Figure 10. Tensile strength (MPa) and elongation at break (%) of the PP/MWNT filaments with different MWNT concentrations.

Conclusion

A method to make PP/MWNT composite using melt-mixing was suggested. Multi-walled carbon nanotubes were first functionalized to have carboxyl group, after then, reacted with MA-g-PP in a xylene/ethanol solvent to make them interact with the non-polar polymer of polypropylene. The functionalized carbon nanotubes were melt-mixed with PP using a twin screw extruder, post-drawn and annealed. SEM and FT-IR analyses showed that the functionalized MWNTs were well dispersed in the non-polar matrix due to the hydrogen bonds between the polymaleic anhydride and MWNT-COOH. The interfacial interaction played also important role in improving the tensile strength of the PP/MWNT composite, which increased at 0.1 wt % MWNT loading by 20 %. In addition, thermal stability and crystallinity were affected by the incorporation of MWNTs. These results suggest that the melt mixing method is effective in preparing PP/MWNT composite.

Acknowledgements

This work was supported by the Soongsil University Research Fund.

References

1. M. J. O'Connell, "Carbon Nanotubes: Properties and Applications", CRC Press, Boca Raton, FL, 2006.
2. S. Kim, B. Min, S. Lee, S. Park, T. Lee, M. Park, and S. Kumar, *Fiber. Polym.*, **5**, 198 (2004).
3. X. Wang, S. Park, K. Yoon, W. Lyoo, and B. Min, *Fiber. Polym.*, **7**, 323 (2006).
4. J. Chen, M. A. Hamon, H. Hu, Y. Chen, A. M. Rao, P. C. Eklund, and R. C. Haddon, *Science*, **282**, 95 (1998).
5. S. Qin, D. Qin, W. T. Ford, D. E. Resasco, and J. E. Herrera, *J. Am. Chem. Soc.*, **126**, 170 (2004).
6. N. R. Raravikar, L. S. Schadler, A. Vijayaraghavan, Y. Zhao, B. Wei, and P. M. Ajayan, *Chem. Mater.*, **17**, 974 (2005).
7. U. S. O. Breuer, *Polym. Compos.*, **25**, 630 (2004).
8. P. J. Boul, J. Liu, E. T. Mickelson, C. B. Huffman, L. M. Ericson, I. W. Chiang, K. A. Smith, D. T. Colbert, R. H. Hauge, J. L. Margrave, and R. E. Smalley, *Chem. Phys. Lett.*, **310**, 367 (1999).
9. B. N. Khare, P. Wilhite, R. C. Quinn, B. Chen, R. H. Schingler, B. Tran, H. Imanaka, C. R. So, C. W. Bauschlicher, and M. Meyyappan, *J. Phys. Chem. B*, **108**, 8166 (2004).

10. V. C. M. Sclavons, B. De Roover, P. Franquinet, J. Devaux, and R. Legras, *J. Appl. Polym. Sci.*, **62**, 1205 (1996).
11. G.-W. Lee, S. Jagannathan, H. G. Chae, M. L. Minus, and S. Kumar, *Polymer*, **49**, 1831 (2008).
12. B. Marosföi, A. Szabó, G. Marosi, D. Tabuani, G. Camino, and S. Pagliari, *J. Therm. Anal. Calorim.*, **86**, 669 (2006).
13. B. Wunderlich, "Thermal Analysis", Academic Press, Boston, 1990.
14. R. J. Young and P. A. Lovell, "Introduction to Polymers", Chapman & Hall, New York, 1994.
15. P. R. Marcoux, J. Schreiber, P. Batail, S. Lefrant, J. Renouard, G. Jacob, D. Albertini, and J.-Y. Mevellec, *Phys. Chem. Chem. Phys.*, **4**, 2278 (2002).
16. J. B. L. Valentini, J. M. Kenny, and M. A. Lopez Manchado, *J. Appl. Polym. Sci.*, **89**, 2657 (2003).